

## 2D segment model for a bi-layer electrolyte solid oxide fuel cell

Shuanglin Shen <sup>a,\*</sup>, Meng Ni <sup>b</sup>

<sup>a</sup> School of Electric Power Engineering, China University of Mining and Technology, Xuzhou, 221116, China

<sup>b</sup> Department of Building and Real Estate, The Hong Kong Polytechnic University, Hung Hom, Kowloon, Hong Kong

\* Corresponding author: Shuanglin Shen

Email: shensln01@163.com; Tel: (086) 15050829069; Fax: (086) 0516-83592000

**Abstract:**

A 2D segment model for a bi-layer electrolyte solid oxide fuel cell (SOFC) is developed by coupling the mass transport in the channel and electrode, electrochemical reaction at the electrode/electrolyte interface and charge transport in the bi-layer electrolyte. The Butler-Volmer equation is used to describe the electrochemical reaction. The expressions of electronic current and oxygen partial pressure in the electrolyte are obtained by the 1D charge transport equation and two additional equations based on energy conservation are derived to close the governing equations. The model is validated as the simulation results agree well with the experiment data reported in the literature. The characteristics of a SOFC with an yttria stabilized zirconia (YSZ)/samaria doped ceria (SDC) bi-layer electrolyte is parametrically analyzed and the uniformity of the electronic current and oxygen partial pressure in SOFC under various operating conditions is investigated. The results provide fundamental information on the leakage current in a bi-layer electrolyte SOFC and can serve as a useful tool for its design optimization.

Keywords: 2D model, bi-layer electrolyte, solid oxide fuel cell, leakage current

## 1. Introduction

A solid oxide fuel cell (SOFC) as an effective electricity generating device has received much attention due to its high power density, high efficiency, low harmful gas emission and fuel flexibility<sup>1</sup>. Acceptor doped ceria (ADC) and stabilized bismuth oxide (SBO) are promising electrolytes for the intermediate temperature (500°C-800 °C) solid oxide fuel cell (ITSOFC) owing to their high ionic conductivity<sup>2-7</sup>. However, at low oxygen partial pressure acceptor doped ceria shows considerable electronic conductivity<sup>8</sup> and stabilized bismuth oxide can decompose<sup>9</sup>, which essentially hinder their application in the ITSOFC. A bi-layer electrolyte, comprising a thin electronic-insulating layer or low oxygen diffusivity layer at the anode side, can block the electronic current and protect the unstable electrolyte from decomposition<sup>10-12</sup>.

The YSZ (Yttria stabilized zirconia)/ADC and ADC/SBO bi-layer electrolytes were mostly studied in the literature. Yahiro et al.<sup>12</sup> experimentally demonstrated that the YSZ/ADC bi-layer electrolyte can effectively block the electronic current and enhance the open-circuit voltage of the fuel cell. Thereafter, many fabrication techniques for the YSZ/ADC bi-layer electrolyte SOFC were proposed in the literatures to improve its performance<sup>13-18</sup>, and the characteristics of the YSZ/ADC bi-layer electrolyte SOFC was experimentally studied<sup>19, 20</sup>. Wachsman et al.<sup>11</sup> first proposed the ADC/SBO bi-layer electrolyte for ITSOFC and experimentally demonstrated that the ADC/SBO bi-layer electrolyte SOFC has much high power density and good chemical stability<sup>10, 21-23</sup> at intermediate temperature.

Except these experimental works, there are also a few of theoretical studies on the bi-layer electrolyte SOFC. Virkar<sup>24</sup> theoretically analyzed the chemical stability of the bi-layer electrolyte by an equivalent circuit model and concluded the effects of the transport properties of the electrolyte on the chemical stability of the bi-layer electrolyte. Marques and Navarro<sup>25, 26</sup> built an oxygen permeation model by developing a series of exact relationship between the transport properties of the electrolyte and the cell oxygen partial pressure profile, voltage and leakage current and analyzed the performance of the YSZ/ADC bi-layer electrolyte. Chan et al.<sup>27</sup> developed a simple bi-layer electrolyte model for SOFC based on the charge transport equation (Nernst-Planck equation) and

theoretically analyzed the effect of the relative thickness of the bi-layer electrolyte on the SOFC performance. Shen et al.<sup>28,29</sup> developed an analytical model for the bi-layer electrolyte SOFC based on the charge transport equation and obtained a series of equations for the relative thickness optimization and useful results for the bi-layer electrolyte design by the parametric analysis.

However, the theoretical studies mentioned-above focus on the characteristics of the bi-layer electrolyte and neglect the effect of the electrochemical reaction and the species concentration. Thus, these numerical models are inapplicable to analyze the practical fuel cell, so in this paper a 2D segment model for a bi-layer electrolyte SOFC is developed by coupling the charge transport in the bi-layer electrolyte with the electrochemical reaction at the triple-phase boundary (TPB) and mass transport in the porous electrodes and gas channels. The model is validated by comparing with the experimental data and then used to analyze the characteristics of a 2D bi-layer electrolyte SOFC.

## **2. 2D segment model for bi-layer electrolyte SOFC**

The 2D schematic of a bi-layer electrolyte SOFC is shown in Fig.1. The fuel cell contains 6 layers including anode channel (AC), anode (AN), electron blocking or protection electrolyte layer (E1, e.g. YSZ), mixed ionic and electronic conducting (MIEC) or unstable electrolyte layer (E2, e.g. ADC or SBO), cathode (CA) and cathode channel (CC). The fuel and air are fed in by the anode and cathode channels respectively, and then diffuse to the electrochemical reaction sites through the porous electrode. The electrochemical reaction is assumed to occur only at the electrode/electrolyte interface, so it is considered as a boundary condition for the charge transport in the electrolyte. The ion yielded in the cathode reaction migrates from cathode to anode and react with the fuel. The electrons produced in the anode reaction mostly migrate to the cathode from the external-circuit meanwhile several electrons leak to the cathode through the bi-layer electrolyte even though there is an electron blocking layer. In this model, several reasonable simplicities are adopted to easily analyze the main characteristics of the bi-layer electrolyte SOFC, those are,

- a) The pressure drop along the gas channel is neglected to avoid the complex momentum conservation, so the constant average inlet velocities,  $u_{an}$  and  $u_{ca}$ , are specified.
- b) The mobile charges in the electrolyte are oxygen ion and electron. The hole migration in the electrolyte is neglect. This assumption is rational for the most MIEC materials at the SOFC

operating conditions since the p-type conductivity MIEC materials used in the SOFC are less common<sup>26</sup>. Besides, it must be pointed out that some MIEC materials may change from n-type conductivity to p-type conductivity as the oxygen partial pressure increases from the anode side to the cathode side (e.g. SBO<sup>30</sup>), and this feature must be considered when this model is applied in those MIEC materials.

- c) The electrochemical reaction is assumed to occur only at the electrode/electrolyte interface, because this model focuses on the leakage current and oxygen partial pressure in the electrolyte and this assumption can much simplified the model calculation and results analysis without change of the qualitative conclusions.
- d) The electrical current in  $x$  direction are neglected, as well as the gas flux, thus, the fuel cell is cut to many equal-width segments along the gas flowing direction and in each segment the gas diffusion and charge transport are considered in one dimension.

### 2.1 Mass transfer

The hydrogen and air are fed in the SOFC by the gas channel, respectively, and then diffuse through the porous electrode to the reaction site. In the gas channel, the mass conservation is considered and the equation of the gas concentration is obtained as:

$$u \frac{\partial c_i}{\partial x} = v_i \frac{j_{O_2}}{2F} \frac{1}{\tau_{\text{Channel}}} \quad i \in \{H_2, O_2, H_2O\} \quad (1)$$

where  $c$  is concentration,  $v$  is stoichiometric coefficient (1 for  $H_2$ , 1/2 for  $O_2$  and -1 for  $H_2O$ ),  $j_{O_2}$  is the oxygen ionic current density,  $F$  is the Faradic constant and  $\tau_{\text{Channel}}$  is the width of the channel (the width of anode and cathode channel is same).

In the anode, the hydrogen diffuses from anode channel to the electrochemical reaction interface; meanwhile the product of the reaction, steam, diffuses from the reaction site to the anode channel. The gas diffusion flux can be obtained by the Faradic law and the gas concentration at the anode/electrolyte interface can be obtained by the equimolar counter-current diffusion equations<sup>31</sup> as,

$$p_{H_2}^I = p_{H_2}^{ac} - \frac{RT \cdot \tau_{an}}{2FD_{\text{eff},an}} j_{O_2} \cdot \delta x \quad (2)$$

$$p_{\text{H}_2\text{O}}^I = p_{\text{H}_2\text{O}}^{\text{ac}} + \frac{RT \cdot \tau_{\text{an}}}{2FD_{\text{eff,an}}} j_{\text{O}_2} \cdot \delta x \quad (3)$$

where  $p_{\text{H}_2}^{\text{ac}}$  and  $p_{\text{H}_2\text{O}}^{\text{ac}}$  are the  $\text{H}_2$  partial pressure and  $\text{H}_2\text{O}$  partial pressure at the anode channel, respectively,  $R$  is the universal gas constant,  $T$  is the temperature,  $\tau_{\text{an}}$  is the anode thickness,  $\delta x$  is the width of a segment and  $D_{\text{eff,an}}$  is the effective diffusivity at the anode and can be calculated by,

$$D_{\text{eff,an}} = \left( \frac{p_{\text{H}_2\text{O}}}{p_0} \right) D_{\text{H}_2,\text{eff}} + \left( \frac{p_{\text{H}_2}}{p_0} \right) D_{\text{H}_2\text{O},\text{eff}} \quad (4)$$

where  $p_0$  is the pressure at the standard state. The hydrogen and steam partial pressures are variable in the anode, consequently the anode effective diffusivity is also variable and gas concentration at the anode/electrode interface can't be calculated directly by Eqs.(2) and (3). For simplicity, the hydrogen and steam partial pressures at the anode channel are substituted into Eq.(4) to calculate the anode effective diffusivity, since the difference between hydrogen and steam effective diffusivities is not very large<sup>31</sup>. The hydrogen and steam effective diffusivities are obtained, respectively, as:

$$\frac{1}{D_{\text{eff,H}_2}} = \frac{\varepsilon}{\tau} \left( \frac{1}{D_{\text{H}_2-\text{H}_2\text{O}}} + \frac{1}{D_{\text{H}_2,\text{k}}} \right) \quad (5)$$

$$\frac{1}{D_{\text{eff,H}_2\text{O}}} = \frac{\varepsilon}{\tau} \left( \frac{1}{D_{\text{H}_2-\text{H}_2\text{O}}} + \frac{1}{D_{\text{H}_2\text{O},\text{k}}} \right) \quad (6)$$

where,  $\varepsilon$  is the porosity,  $\tau$  is the tortuosity factor,  $D_{\text{H}_2-\text{H}_2\text{O}}$  is the binary diffusivity of  $\text{H}_2$  and  $\text{H}_2\text{O}$  and  $D_{i,\text{k}}$  is the Knudsen diffusivity ( $i$  is  $\text{H}_2$  or  $\text{H}_2\text{O}$ ).  $D_{\text{H}_2-\text{H}_2\text{O}}$  and  $D_{i,\text{k}}$  can be calculated by Fuller et al. expression<sup>32,33</sup> and gases kinetic theory<sup>34</sup>, respectively.

In the cathode, only the oxygen diffuses from cathode channel to the cathode/electrolyte interface, thus the oxygen partial pressure at the interface can be obtained by the self-diffusion equation<sup>31</sup> as,

$$p_{\text{O}_2}^{\text{II}} = \frac{p_0}{f_d} - \left( \frac{p_0}{f_d} - p_{\text{O}_2}^{\text{cc}} \right) \exp \left( \frac{f_d RT \cdot \tau_{\text{ca}}}{4FD_{\text{eff,O}_2} p_0} j_{\text{O}_2} \cdot \delta x \right) \quad (7)$$

where, the effective oxygen diffusivity  $D_{\text{eff},\text{O}_2}$  is obtained by combing the binary diffusivity of  $\text{O}_2$  and  $\text{N}_2$  and the Knudsen diffusivity of  $\text{O}_2$  as,

$$\frac{1}{D_{\text{eff},\text{O}_2}} = \frac{\varepsilon}{\tau} \left( \frac{1}{D_{\text{O}_2\text{-N}_2}} + \frac{1}{D_{\text{O}_2,\text{k}}} \right) \quad (8)$$

and the coefficient  $f_d$  is defined by,

$$f_d = \frac{D_{\text{O}_2,\text{k}}}{D_{\text{O}_2,\text{k}} + D_{\text{O}_2\text{-N}_2}} .$$

## 2.2 Electrochemical reaction

The electrochemical reaction at the electrode/electrolyte interface is described by the Butler-Volmer equation as,

$$\text{Anode:} \quad j_{\text{O}^{2-}} = j_{0,\text{an}} \left\{ \frac{p_{\text{H}_2}^I}{p_{\text{H}_2}^{\text{ref}}} \exp\left(\alpha_{\text{an}} \frac{nF}{RT} \eta_{\text{an}}\right) - \frac{p_{\text{H}_2\text{O}}^I}{p_{\text{H}_2\text{O}}^{\text{ref}}} \exp\left[-(1-\alpha_{\text{an}}) \frac{nF}{RT} \eta_{\text{an}}\right] \right\} \quad (9)$$

$$\text{Cathode:} \quad j_{\text{O}^{2-}} = j_{0,\text{ca}} \left\{ \exp\left(\alpha_{\text{ca}} \frac{nF}{RT} \eta_{\text{ca}}\right) - \exp\left[-(1-\alpha_{\text{ca}}) \frac{nF}{RT} \eta_{\text{ca}}\right] \right\} \frac{p_{\text{O}_2}^{II}}{p_{\text{O}_2}^{\text{ref}}} \quad (10)$$

where,  $j_0$  is the exchange current density,  $p_i^{\text{ref}}$  is the reference partial pressure of species  $i$  (1 bar for all species),  $\alpha$  is the transfer coefficient and  $\eta$  is the electrode overpotential. The electrode overpotential  $\eta$  can be obtained as,

$$\eta = E_{\text{rev, an or ca}} - |V_{\text{an or ca}} - \phi_{\text{an or ca}}| \quad (11)$$

where  $E_{\text{rev}}$  is the reversible electrode potential,  $V$  is the electrode potential and  $\phi$  is the electrical potential in the electrolyte.

The voltages at the anode and cathode are specified to 0 and  $V$ , respectively. The ohmic losses in the electrodes are neglected duo to the high electrical conductivity of the electrode. Thus the polarization equation for the SOFC with MIEC electrolyte can be obtained by the energy conservation analysis as<sup>35</sup>,

$$j_L V = j_{\text{O}^{2-}} E_{\text{th}} - j_{\text{O}^{2-}} (\eta_{\text{an}} + \eta_{\text{ca}}) - j_{\text{O}^{2-}} \eta_{\text{ohm},\text{O}^{2-}} - |j_e| \eta_{\text{ohm},\text{e}} - j_{\text{O}^{2-}} \eta_{\text{conc}} \quad (12)$$

where,  $j_L$  is the load (or output) current density,  $E_{th}$  is the Nernst potential,  $\eta_{ohm,O^{2-}}$  is the ohmic loss for the oxygen ion conduction,  $j_e$  is the electronic leakage current density in the electrolyte,  $\eta_{ohm,e}$  is the ohmic loss for the electronic leakage current and  $\eta_{conc}$  is the concentration loss.

The relation of the output, ionic and electronic current densities can be obtained by the Kirchhoff law as,

$$j_L = j_{O^{2-}} + j_e \quad (13)$$

### 2.3 Charge transport in the bi-layer electrolyte

The charge transport in the bi-layer electrolyte was studied by previous theoretical model<sup>29</sup> and the expressions of the ionic and electronic current densities and oxygen partial pressure in the electrolyte can be applied in this model by neglecting the slight electrical current in  $x$  direction. Thus, the ionic and electronic current densities in each segment can be obtained as,

$$j_{O^{2-}} = -\frac{\sigma_{O^{2-}}^{eq}}{L} \Delta\phi \quad (14)$$

$$j_e = -\frac{\sigma_{O^{2-}}^{eq}}{L} \frac{M_1 (p_{O_2}^0)^{-1/4} - \frac{1}{M_2} (p_{O_2}^L)^{-1/4}}{(M_1 - 1) \frac{\sigma_{O^{2-}}^{E1}}{\sigma_e^{0,E1}} + \left(1 - \frac{1}{M_2}\right) \frac{\sigma_{O^{2-}}^{E2}}{\sigma_e^{0,E2}}} \Delta\phi \quad (15)$$

where,  $\phi$  is the electrical potential in the electrolyte,  $L$  is the total thickness of the bi-layer electrolyte and  $\sigma_{O^{2-}}^{eq}$  is the equivalent ionic conductivity of the bi-layer electrolyte and defined as,

$$\sigma_{O^{2-}}^{eq} = \frac{L}{s_1 / \sigma_{O^{2-}}^{E1} + s_2 / \sigma_{O^{2-}}^{E2}} \quad (16)$$

$\sigma_{O^{2-}}^{E1}$ ,  $\sigma_{O^{2-}}^{E2}$ ,  $\sigma_e^{0,E1}$  and  $\sigma_e^{0,E2}$  are the ionic conductivity and electronic conductivity of electrolyte 1 and electrolyte 2, respectively. The intermediate variables,  $M_1$  and  $M_2$  are defined as,

$$M_1 = \exp\left(-\frac{F}{RT} \frac{j_{O^{2-}}}{\sigma_{O^{2-}}^{E1}} s_1\right), \quad M_2 = \exp\left(-\frac{F}{RT} \frac{j_{O^{2-}}}{\sigma_{O^{2-}}^{E2}} s_2\right)$$

where  $s_1$  and  $s_2$  are the thicknesses of the E1 and E2 respectively.

The oxygen partial pressure in the bi-layer electrolyte also can be obtained as,

$$[p_{O_2}(y)]^{-1/4} = (p_{O_2}^0)^{-1/4} \exp\left(-\frac{F}{RT} \frac{j_{O_2^{2-}}}{\sigma_{O_2^{2-}}^{E1}} y\right) - \frac{j_e \sigma_{O_2^{2-}}^{E1}}{j_{O_2^{2-}} \sigma_e^{0,E1}} \left[ \exp\left(-\frac{F}{RT} \frac{j_{O_2^{2-}}}{\sigma_{O_2^{2-}}^{E1}} y\right) - 1 \right], \quad (0 < y < s_1) \quad (17)$$

$$[p_{O_2}(y)]^{-1/4} = (p_{O_2}^L)^{-1/4} \exp\left[-\frac{F}{RT} \frac{j_{O_2^{2-}}}{\sigma_{O_2^{2-}}^{E2}} (y-L)\right] - \frac{j_e \sigma_{O_2^{2-}}^{E2}}{j_{O_2^{2-}} \sigma_e^{0,E2}} \left\{ \exp\left[-\frac{F}{RT} \frac{j_{O_2^{2-}}}{\sigma_{O_2^{2-}}^{E2}} (y-L)\right] - 1 \right\}, \quad (s_1 < y < L). \quad (18)$$

In order to calculate the electronic current density and oxygen partial pressure in the bi-layer electrolyte, the boundary oxygen partial pressure at  $y=0$  and  $L$  must be given or calculated first. Thus, the relationships between oxygen partial pressure at the electrode (the given operating condition) and that at the electrolyte boundary are required. According to the previous energy conservation analysis based on Eq.(11)<sup>35</sup>, The boundary oxygen partial pressure at the anode side is obtained as,

$$\frac{RT}{4F} \ln \frac{p_{O_2}^L}{p_{O_2}^0} = V - \Delta\phi \quad (19)$$

If the cathode half-reaction is only considered and the anode is assumed as a ideally non-polarizable electrode, thus substituting Eq.(11) into Eq.(19), the expression of the boundary oxygen partial pressure at the cathode side is obtained as,

$$\frac{RT}{4F} \ln p_{O_2}^L = \frac{RT}{4F} \ln p_{O_2}^{II} - \eta_{ca} . \quad (20)$$

In the same way, if only the anode half-reaction is considered, the expression of the boundary oxygen partial pressure at the anode side is obtained as,

$$\frac{RT}{4F} \ln p_{O_2}^0 = \eta_{an} + \frac{RT}{4F} \ln p_{O_2}^I . \quad (21)$$

The oxygen partial pressure at the anode/electrode interface is obtained by the mass action law of the water reaction as,

$$K_{eq} = \frac{p_{H_2O}^I}{p_{H_2}^I \sqrt{p_{O_2}^I}} \quad (22)$$

where  $K_{eq}$  is the equilibrium constant of water steam.

### 3. Model validation

The model is validated by comparing the model results with experiment data reported in 19, in which a Ni-YSZ||YSZ|SDC||LSCF ( $\text{La}_{0.6}\text{Sr}_{0.4}\text{Co}_{0.2}\text{Fe}_{0.8}\text{O}_3$ ) bi-layer electrolyte SOFC was fabricated by pulsed laser deposition technique. The thickness of YSZ and SDC are 0.7  $\mu\text{m}$  and 5  $\mu\text{m}$  respectively, and the thickness of the anode and cathode are about 1 mm and 50 mm respectively. The conductivity parameters for the SDC electrolyte are measured in the previous experiment and listed in Table 1. The ionic conductivity of the YSZ is calculated by the equation,  $3.34 \times 10^6 \exp(-10300/T)$  S/cm<sup>36</sup>, while the electronic conductivity of the YSZ is dependent on the -1/4 power of the local oxygen partial pressure and the coefficient is calibrated in the program to fitting the experiment data. The exchange current densities of anode and cathode are also the fitting parameters in the program and the final value of the fitting parameters in the program are listed in Table 2. Besides, the ohmic losses caused by the contact resistance, electrode resistance and system resistance are included in the model by the ohmic law and the sum of these resistance is estimated by the EIS (Electrochemical Impedance Spectroscopy) results<sup>19</sup> as,

$$R_{other} = R_{EIS} - \frac{\tau_{E1}}{\sigma_{O^{2-}}^{E1}} - \frac{\tau_{E2}}{\sigma_{O^{2-}}^{E2}} \quad (23)$$

where  $R_{EIS}$  is the ohmic resistance measured by the EIS. The estimated results are listed in Table 3. The other parameters used in the program are listed in Table 4.

The comparison results are shown in the Fig.2. The model results agree well with the experiment data at different operating temperature and this indicates that this model can reliably estimate the performance of the bi-layer electrolyte SOFC with proper parameters and can be used to analyze the characteristics of the bi-layer electrolyte SOFC and assist its design.

#### 4. The analysis on a bi-layer electrolyte SOFC

The YSZ|SDC bi-layer electrolyte is mostly fabricated in the literature, but there is lack of theoretical analysis on the bi-layer electrolyte SOFC, especially the uniformity problem. In this paper, the distribution characteristics of a 3  $\mu\text{m}$ YSZ|27  $\mu\text{m}$  SDC bi-layer electrolyte SOFC is studied by the 2D segment model with varied inlet velocities. The thickness of the anode and cathode are 700  $\mu\text{m}$  and 20  $\mu\text{m}$ , respectively. The width and length of the gas channel are 1 mm and 50 mm respectively. The parameters of the SDC and YSZ and exchange current densities used in the analysis are same to

these used in the validation program. The temperature of whole cell is considered uniform and equal to 700°C. The anode feed gas comprises by 97 Vol.% H<sub>2</sub> and 3 Vol.% steam and the cathode is fed by air.

#### *4.1 The whole performance of the bi-layer electrolyte SOFC*

The polarization curves and power density curves of the bi-layer electrolyte SOFC with different gas inlet velocities are shown in Fig.3. Comparing with the performance of SOFC with SDC electrolyte<sup>35</sup>, the bi-layer electrolyte SOFC shows the higher open-circuit voltage, this implies that the YSZ layer can effectively block the leakage current. The dependency of the performance of the bi-layer electrolyte SOFC on the gas inlet velocity is similar to that of the SOFC with YSZ electrolyte<sup>38</sup>, and the performance of the SOFC decreases as the gas inlet velocity decreases due to the concentration loss, especially at the large output current density.

The dependency of average electronic current density of the bi-layer electrolyte SOFC on the operating voltage with different inlet velocities are shown in Fig.4. The electronic current density increases with the increase of the operating voltage and reaches its maximum at open circuit. At an operating voltage, the electronic current density decreases as the fuel inlet velocity decreases, and this indicates that the leakage current can be further suppressed by elevating the fuel utilization ratio. The effect of the air inlet velocity on the average electronic current density is insignificant shown in Fig.4.

#### *4.2 The distribution of the current along gas channel*

The distribution of the output, ionic and electronic current densities along the gas channel with different gas inlet velocities at 0.95 V is shown in Fig.5. The magnitude of the current density all decreases gradually from the inlet to the outlet and this indicates the nonuniformity of the electrochemical reaction along gas channel. For the bi-layer electrolyte SOFC, the decrease of the electronic current density from inlet to outlet can aggravate the nonuniformity of the electrochemical reaction, thus the uniformity problem for the bi-layer electrolyte SOFC must consider seriously in its design.

The effects of the fuel inlet velocity on the distribution of output, ionic and electronic current densities are similar shown in Fig.5, and these current densities decrease with the decrease of the fuel inlet velocity. These results indicate that it will make the uniformity problem much worse to

increase the fuel utilization ratio and the nonuniformity of the electronic current can enlarge this effect. The effect of the air inlet velocity on the current distribution is insignificant.

The distribution of the output, ionic and electronic current densities along the gas channel at a smaller operating voltage, 0.8 V, is shown in Fig.6. Comparing with the results shown in Fig.5, the difference between output current density and ionic current density becomes small with the operating voltage due to the decrease of the electronic current density. This result indicates that the effect of electronic current on the uniformity of electrochemical reaction is important only at a higher operating voltage and this feature makes the nonuniformity of the electrochemical reaction serious even at a high operating voltage (small output current density) if the leakage current is suppressed poorly.

#### *4.3 The distribution of the oxygen partial pressure*

The chemical stability of the SOFC depends on the oxygen partial pressure in the electrolyte and the bi-layer electrolyte can increase the oxygen partial pressure in the electrolyte near the cathode. The analysis on the distribution of the oxygen partial pressure in the bi-layer electrolyte with different gas inlet velocities is also conducted by this model and the results are shown in Fig.7. The YSZ layer can effectively improve the oxygen partial pressure in the SDC layer shown in Fig.7 and according to this characteristic the bi-layer electrolyte can be used to protect the unstable electrolyte such as stabilized bismuth oxide. The oxygen partial pressure in both electrolyte layers increases with the decrease of the fuel inlet velocity shown in Fig.7a, while the effect of the air inlet velocity on the distribution of the oxygen partial pressure is insignificant shown in Fig.7b.

To clearly analyze the characteristics of oxygen partial pressure distribution, two profiles of the oxygen partial pressure at the electrolyte interface ( $y=3 \mu\text{m}$ ) and the middle of the gas channel ( $x=2.5 \text{ cm}$ ) are shown in Fig.8 and Fig.9, respectively. The oxygen partial pressure increases from the inlet to the outlet shown in Fig.8 and the decrease of the fuel inlet velocity can improve the oxygen partial pressure, especially at the downstream of the gas channel. The plotting of the oxygen partial pressure to  $y$  at the middle of the gas channel is similar to the results given in the previous theoretical model<sup>29</sup>. The effect of the gas inlet velocity on the distribution of oxygen partial pressure across the electrolyte is slight and this result implies that for the normal bi-layer electrolyte SOFC, the chemical

stability of the electrolyte at cathode side is independent on the gas distribution which may vary with the operating parameters.

## **5. Conclusions**

A 2D segment model for a bi-layer electrolyte SOFC is developed by combining the gas transfer, electrochemical reaction and charge transport. The gas transfer in the channel is included with a constant gas velocity and the gas diffusion in the anode and cathode are considered by two 1D diffusion equations respectively. The electrochemical reaction at the electrode/electrolyte interface is described by the Butler-Volmer equation. The electrical current in the gas flowing direction is neglected, so a 1D charge transport in the bi-layer electrolyte is considered and the expressions for the current density and oxygen partial pressure obtained in the previous model<sup>29</sup> are introduced in this 2D segment model. The model is validated by comparing with experiment data reported in the literature<sup>19</sup> and well agreement is achieved. The analysis on a YSZ|SDC bi-layer electrolyte SOFC is conducted by this model and the results shown that the YSZ layer can effectively block the leakage current and improve the oxygen partial pressure in the cathode side electrolyte; the decrease of the fuel inlet velocity (increase of the fuel utilization ratio) can slightly suppress the leakage current density but aggravate the nonuniformity of the electrochemical reaction along the gas channel, especially at a higher operating voltage; the effect of the fuel inlet velocity on the distribution of oxygen partial pressure is slight and the effect of the air inlet velocity is insignificant.

## **6. Acknowledgement**

This work was supported by the Fundamental Research Funds for the Central Universities (China University of Mining and Technology). This research was also supported by a grant (Project Number: PolyU 5326/12E) from Research Grant Council, University Grants Committee, Hong Kong SAR.

## Nomenclature:

$c_i$	Concentration of species $i$ , mol cm <sup>-3</sup>
$D$	Diffusivity, m <sup>2</sup> s <sup>-1</sup>
$E_{\text{rev}}$	Reversible potential of the electrode, V
$E_{\text{th}}$	Nernst potential of the fuel cell, V
$F$	Faradic constant, 96485 C mol <sup>-1</sup>
$j_i$	Current density of charge $i$ , A cm <sup>-2</sup>
$K$	Equilibrium constant
$n$	The number of electron transfer in the electrochemical reaction
$p$	Pressure, atm
$R$	Gas constant, 8.314 J mol <sup>-1</sup> K <sup>-1</sup>
$s_i$	Thickness of electrolyte $i$ , m
$T$	Temperature, K
$u$	Gas velocity, m s <sup>-1</sup>
$v_i$	Stoichiometry ratio of species $i$
$x$	Spatial variable in the gas flow direction, m
$y$	Spatial variable across the electrolyte, m

### *Greek symbol*

$\alpha$	Transfer coefficient
$\delta$	Thickness, m
$\varepsilon$	Porosity
$\eta$	Overpotential, V
$\sigma$	Conductivity, S m <sup>-1</sup>
$\tau$	Tortuosity factor
$\tau_i$	The thickness of component $i$ , m
$\phi$	Static electrical potential, V

### *Superscript*

$0$	The parameters at the anode side boundary of the electrolyte
$L$	The parameters at the cathode side boundary of the electrolyte
$I$	The parameters at the anode/electrolyte interface
$II$	The parameters at the cathode/electrolyte interface
ref	The reference parameter
int	The parameters at the interface of the bi-layer electrolyte
E1	Electrolyte 1
E2	Electrolyte 2

*Subscript*

$0$	The parameter at standard state
an	The anode
ac	The anode channel
el	The electrolyte
ca	The cathode
cc	The cathode channel
e	Electron
$H_2$	Hydrogen
$H_2O$	Water
$O_2$	Oxygen
$O^{2-}$	Oxygen ion
eff	Effective

## Reference:

1. S. C. Singhal and K. Kendal, *High Temperature Solid Oxide Fuel Cells: Fundamentals, Design and Applications*, Elsevier, Oxford (2003).
2. J. W. Fergus, *J. Power Sources*, 162, 30 (2006).
3. B. Dalslet, P. Blennow, P. Hendriksen, N. Bonanos, D. Lybye and M. Mogensen, *J. Solid State Electrochem.*, 10, 547 (2006).
4. B. C. H. Steele, *Solid State Ionics*, 129, 95 (2000).
5. H. Inaba and H. Tagawa, *Solid State Ionics*, 83, 1 (1996).
6. N. M. Sammes, G. A. Tompsett, H. Näge and F. Aldinger, *J. Eur. Ceram. Soc.*, 19, 1801 (1999).
7. P. Shuk, H. D. Wiemhöfer, U. Guth, W. Göpel and M. Greenblatt, *Solid State Ionics*, 89, 179 (1996).
8. M. Mogensen, N. M. Sammes and G. A. Tompsett, *Solid State Ionics*, 129, 63 (2000).
9. A. M. Azad, S. Larose and S. A. Akbar, *J. Mater. Sci.*, 29, 4135 (1994).
10. E. D. Wachsman and K. T. Lee, *Science*, 334, 935 (2011).
11. E. D. Wachsman, P. Jayaweera, N. Jiang, D. M. Lowe and B. G. Pound, *J. Electrochem. Soc.*, 144, 233 (1997).
12. H. Yahiro, Y. Baba, K. Eguchi and H. Arai, *J. Electrochem. Soc.*, 135, 2077 (1988).
13. M. Matsuda, T. Hosomi, K. Murata, T. Fukui and M. Miyake, *J. Power Sources*, 165, 102 (2007).
14. Q. L. Liu, K. A. Khor, S. H. Chan and X. J. Chen, *J. Power Sources*, 162, 1036 (2006).
15. C. Brahim, A. Ringuedé, E. Gourba, M. Cassir, A. Billard and P. Briois, *J. Power Sources*, 156, 45 (2006).
16. S.-G. Kim, S. P. Yoon, S. W. Nam, S.-H. Hyun and S.-A. Hong, *J. Power Sources*, 110, 222 (2002).
17. W. S. Jang, S. H. Hyun and S. G. Kim, *J. Mater. Sci.*, 37, 2535 (2002).
18. K. Mehta, R. Xu and A. V. Virkar, *J. Sol-Gel Sci. Technol.*, 11, 203 (1998).
19. Z. Lu, J. Hardy, J. Templeton, J. Stevenson, D. Fisher, N. Wu and A. Ignatiev, *J. Power Sources*, 210, 292 (2012).

20. S. Cho, Y. Kim, J.-H. Kim, A. Manthiram and H. Wang, *Electrochim. Acta*, 56, 5472 (2011).
21. K. T. Lee, D. W. Jung, M. A. Camaratta, H. S. Yoon, J. S. Ahn and E. D. Wachsman, *J. Power Sources*, 205, 122 (2012).
22. J. S. Ahn, D. Pergolesi, M. A. Camaratta, H. Yoon, B. W. Lee, K. T. Lee, D. W. Jung, E. Traversa and E. D. Wachsman, *Electrochem. Commun.*, 11, 1504 (2009).
23. J.-Y. Park, H. Yoon and E. D. Wachsman, *J. Am. Ceram. Soc.*, 88, 2402 (2005).
24. A. V. Virkar, *J. Electrochem. Soc.*, 138, 1481 (1991).
25. F. M. B. Marques and L. M. Navarro, *Solid State Ionics*, 100, 29 (1997).
26. F. M. B. Marques and L. M. Navarro, *Solid State Ionics*, 90, 183 (1996).
27. S. H. Chan, X. J. Chen and K. A. Khor, *Solid State Ionics*, 158, 29 (2003).
28. S. Shen, L. Guo and H. Liu, *Int. J. Hydrogen Energy*, 38, 13084 (2013).
29. S. Shen, L. Guo and H. Liu, *Int. J. Hydrogen Energy*, 38, 1967 (2013).
30. T. Takahashi, T. Esaka and H. Iwahara, *J. Appl. Electrochem.*, 7, 303 (1977).
31. S. H. Chan, K. A. Khor and Z. T. Xia, *Journal of Power Sources*, 93, 130 (2001).
32. G. Karaiskakis and D. Gavril, *Journal of Chromatography A*, 1037, 147 (2004).
33. B. Todd and J. B. Young, *J. Power Sources*, 110, 186 (2002).
34. M. Ni, *Int. J. Hydrogen Energy*, 36, 3153 (2011).
35. S. Shen, Y. Yang, L. Guo and H. Liu, *J. Power Sources*, 256, 43 (2014).
36. P. Aguiar, C. S. Adjiman and N. P. Brandon, *J. Power Sources*, 138, 120 (2004).
37. M. Ni, *Int. J. Hydrogen Energy*, 38, 2846 (2013).
38. J. Milewski, K. Świrski, M. Santarelli and P. Leone, *Advanced Methods of Solid Oxide Fuel Cell Modeling*, Springer, New York (2011).

### **List of the Tables:**

**Table 1.** The conductivity of the SDC

**Table 2.** The fitting parameters in the model

**Table 3.** The sum of the other resistances

**Table 4.** The parameters used in the model calculation<sup>37</sup>

### **List of the Figures:**

**Figure 1.** The 2D schematic of a bi-layer electrolyte SOFC

**Figure 2.** The comparison of the model results with experiment data in 19

**Figure 3.** The polarization curves and power density curves of the bi-layer electrolyte SOFC with different inlet velocities

**Figure 4.** The electronic current density of the bi-layer electrolyte SOFC with different inlet velocities

**Figure 5.** The distribution of the current densities along the gas channel at 0.95 V

**Figure 6.** The distribution of the current densities along the gas channel at 0.8 V

**Figure 7.** The distribution of oxygen partial pressure in the bi-layer electrolyte with different inlet velocity

**Figure 8.** The plotting of the oxygen partial pressure to x at the electrolyte interface ( $y=3 \mu\text{m}$ )

**Figure 9.** The plotting of the oxygen partial pressure to y at the middle of the gas channel ( $x=2.5 \text{ cm}$ )

Table 1 the conductivity of the SDC

	600°C	650°C	700°C
Ionic / $\text{Scm}^{-1}$	0.0112	0.0193	0.0332
Electronic coefficient / $\text{Scm}^{-1}$	1.96E-8	8.21E-8	2.77E-7

Table 2 the fitting parameters in the model

	600°C	650°C	700°C
Anode exchange current density / $\text{Am}^{-2}$	1450	2900	4500
Cathode exchange current density / $\text{Am}^{-2}$	830	1850	2950
Electronic coefficient of YSZ / $\text{Scm}^{-1}$	4.0E-11	2.8E-10	7.5E-10

Table 3 the sum of the other resistances

	600°C	650°C	700°C
Scm <sup>-1</sup>	7.9E-6	6.1E-6	5.3E-6

Table 4 the parameters used in the model calculation<sup>37</sup>

Parameter	Value
Operating pressure, $p_0$ (bar)	1.0
Electrode porosity, $\varepsilon$	0.4
Electrode tortuosity factor, $\tau$	3.0
Average pore radius of the electrode, ( $\mu\text{m}$ )	0.5
Anode inlet gas molar ratio, $\text{H}_2/\text{H}_2\text{O}$	0.97/0.03
Cathode inlet gas molar ratio, $\text{O}_2/\text{N}_2$	0.21/0.79
Reference pressure, $p^{\text{ref}}$ (bar)	1.0
Transfer coefficient, $\alpha$	0.5
Number of transfer electrons, n	2



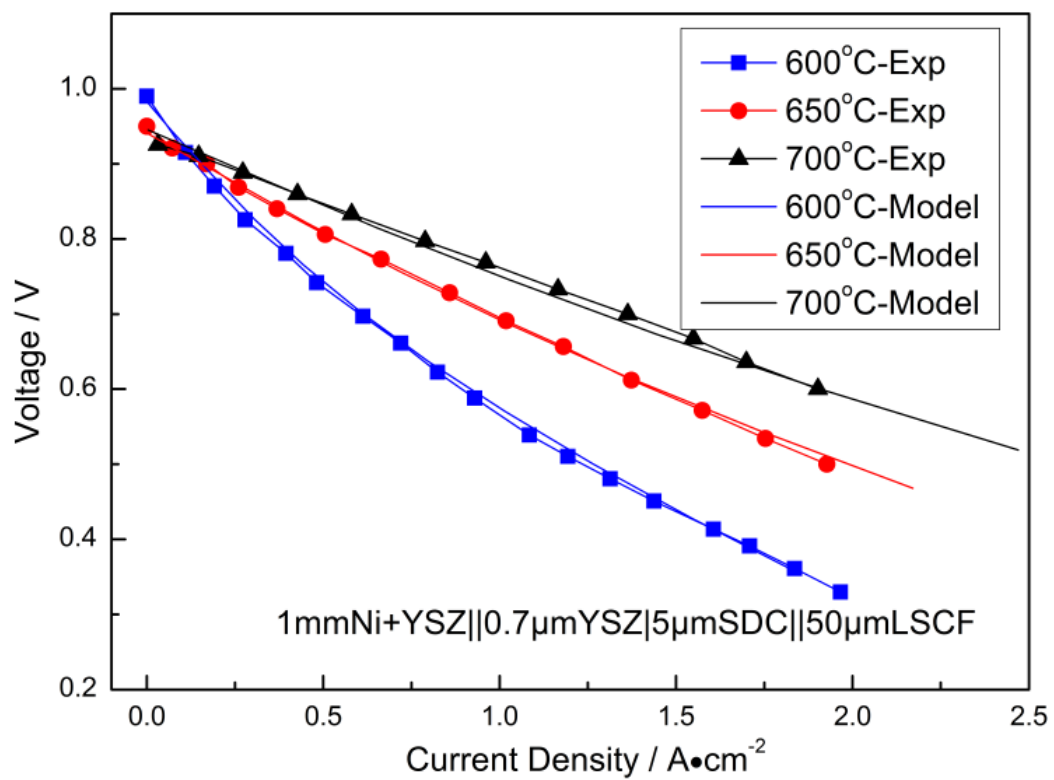


Fig.2 The comparison of the model results with experiment data in 19

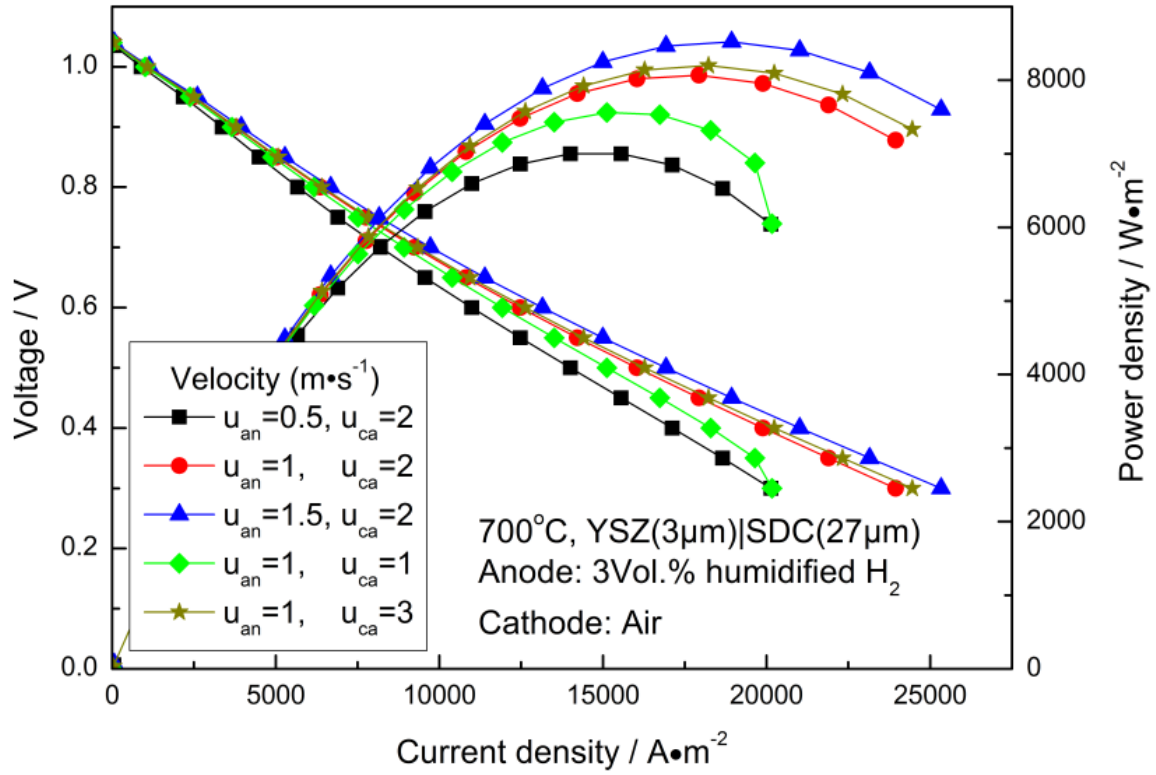


Fig.3 The polarization curves and power density curves of the bi-layer electrolyte SOFC with different inlet velocities

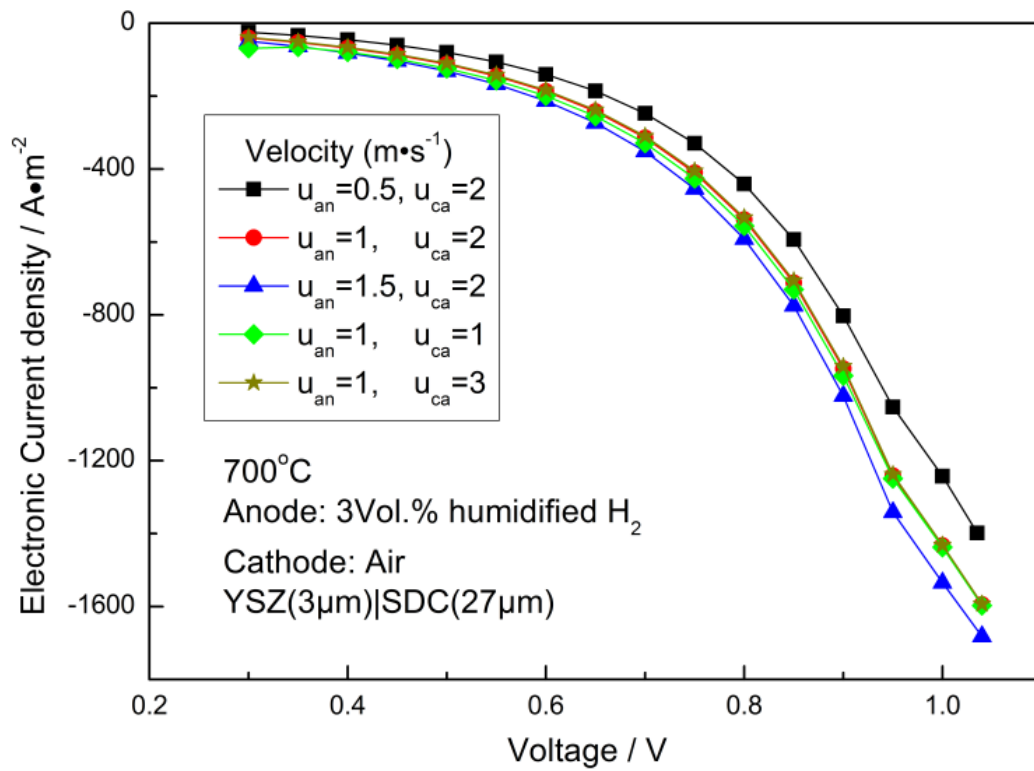


Fig.4 The electronic current density of the bi-layer electrolyte SOFC with different inlet velocities

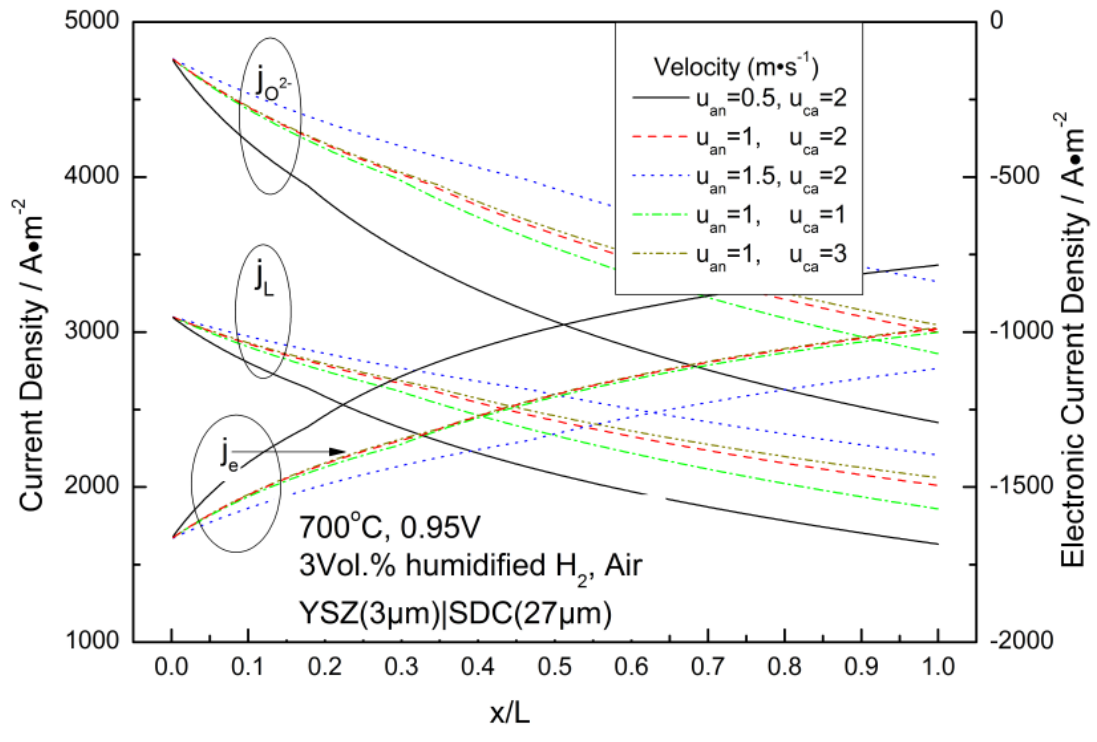


Fig.5 The distribution of the current densities along the gas channel at 0.95 V

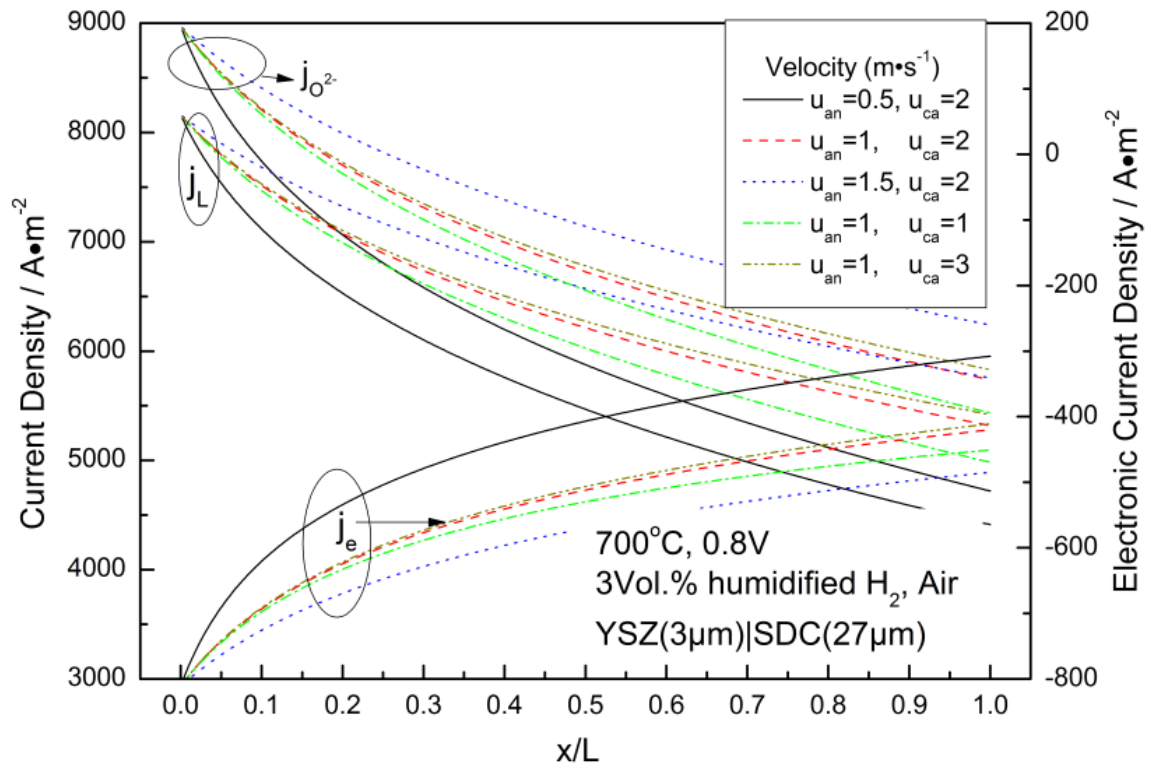


Fig.6 The distribution of the current densities along the gas channel at 0.8 V

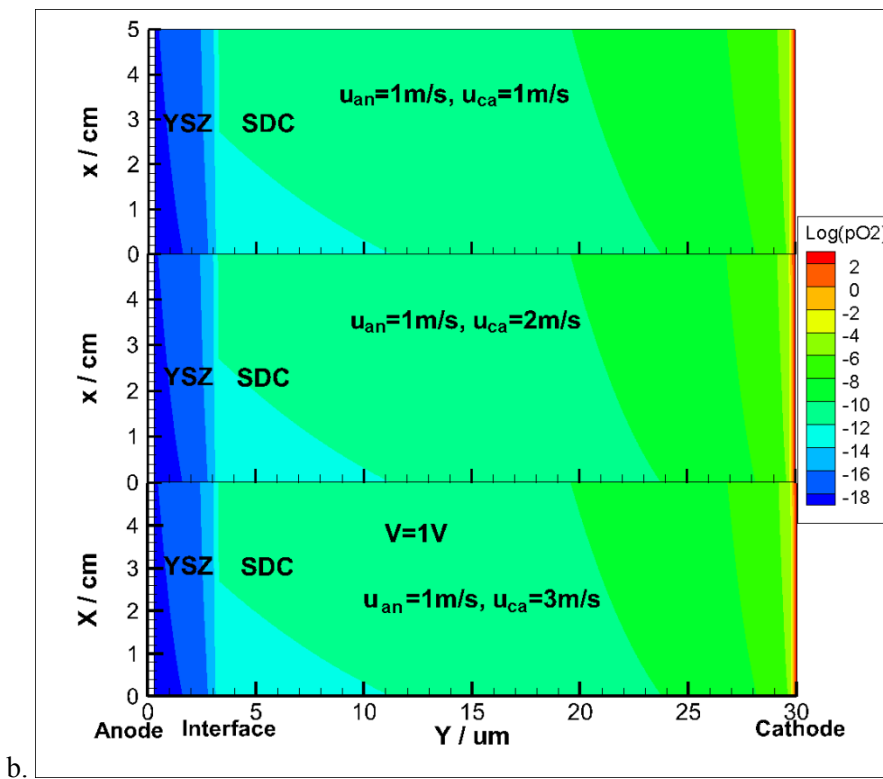
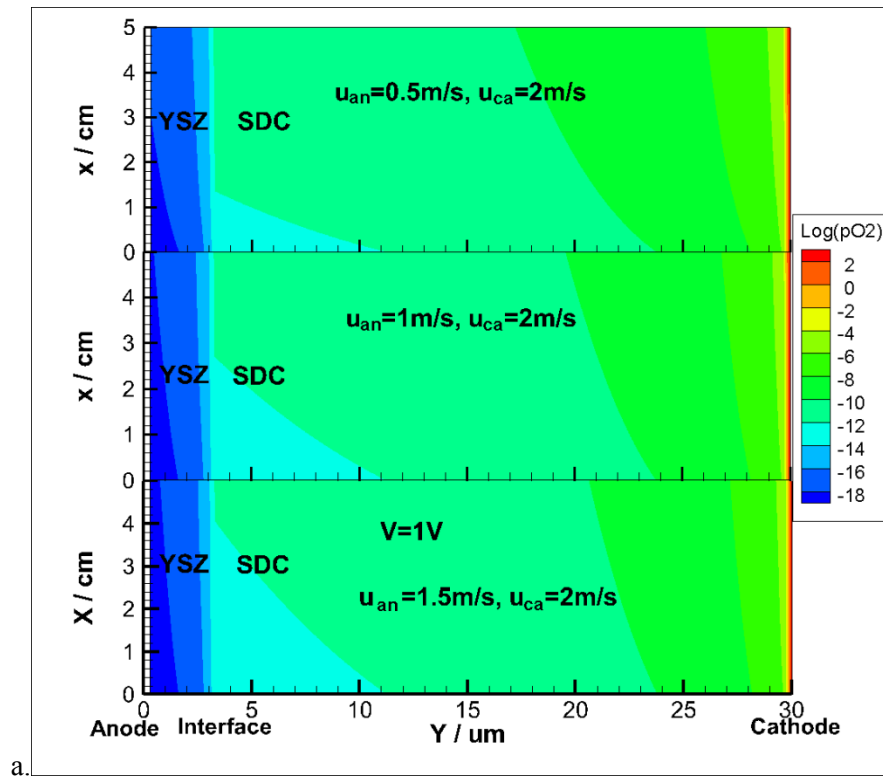


Fig.7 The distribution of oxygen partial pressure in the bi-layer electrolyte with different inlet velocity

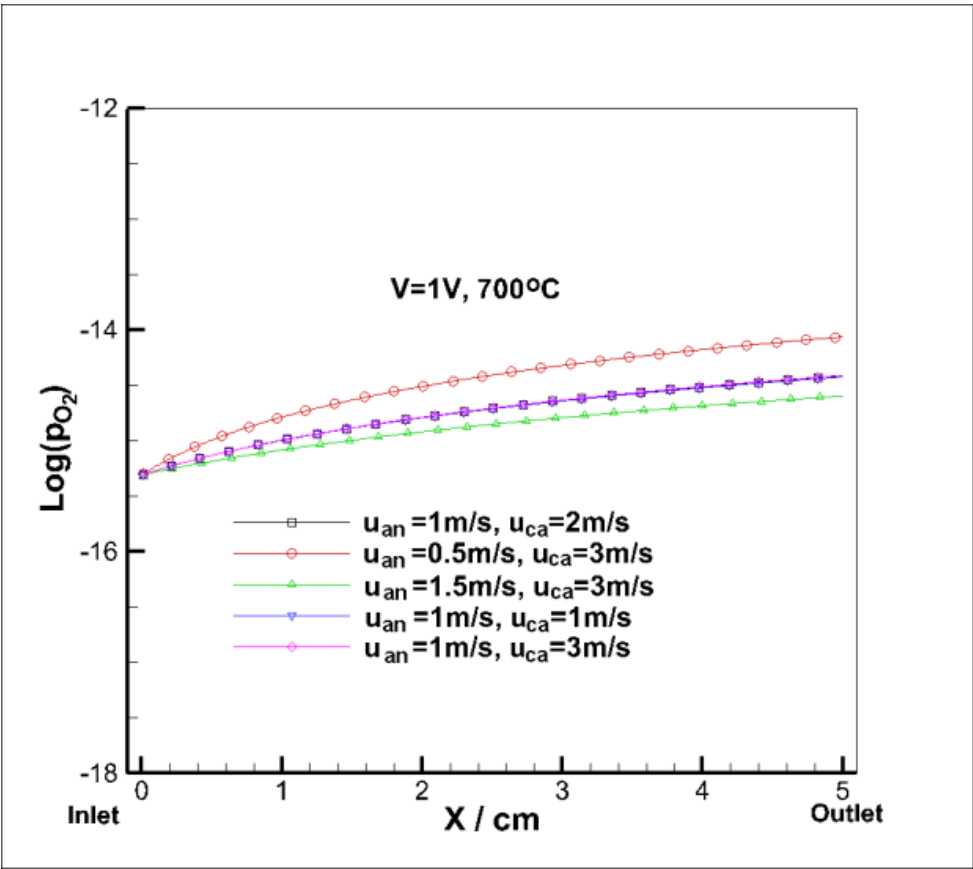


Fig.8 The plotting of the oxygen partial pressure to x at the electrolyte interface ( $\gamma=3 \mu\text{m}$ )

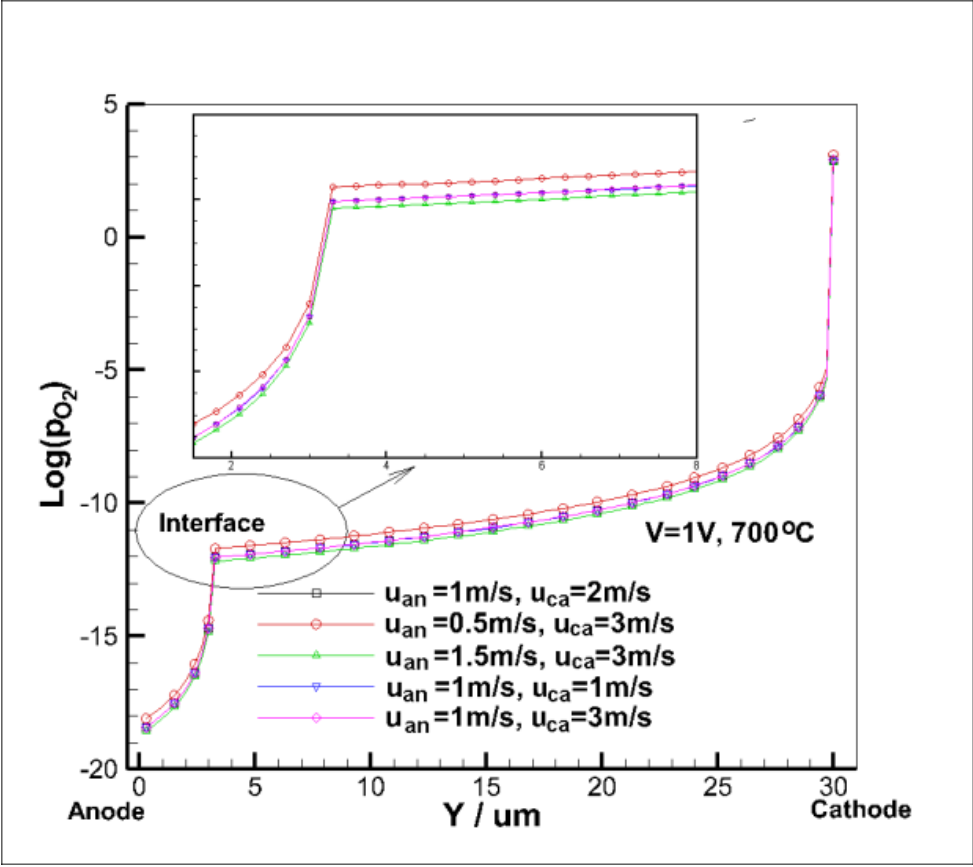


Fig.9 The plotting of the oxygen partial pressure to  $y$  at the middle of the gas channel ( $x=2.5$  cm)